

Effect of nonequilibrium phonons on hot-electron spin relaxation in n -type GaAs quantum wells

P. Zhang and M. W. Wu*

*Hefei National Laboratory for Physical Sciences at Microscale and Department of Physics,
University of Science and Technology of China, Hefei, Anhui, 230026, China*

(Dated: April 2, 2024)

We have studied the effect of nonequilibrium longitudinal optical phonons on hot-electron spin relaxation in n -type GaAs quantum wells. The longitudinal optical phonons, due to the finite relaxation rate, are driven to nonequilibrium states by electrons under an in-plane electric field. The nonequilibrium phonons then in turn influence the electron spin relaxation properties via modifying the electron heating and drifting. The spin relaxation time is elongated due to the enhanced electron heating and thus the electron-phonon scattering in the presence of nonequilibrium phonons. The frequency of spin precession, which is roughly proportional to the electron drift velocity, can be either increased (at low electric field and/or high lattice temperature) or decreased (at high electric field and/or low lattice temperature). The nonequilibrium phonon effect is more pronounced when the electron density is high and the impurity density is low.

PACS numbers: 72.25.Rb, 71.10.-w, 63.20.kd

I. INTRODUCTION

Understanding spin relaxation is an important issue for the possible application of spintronic devices.^{1–4} Among different kinds of spin relaxation mechanisms,^{5–7} scattering plays an essential role. In general cases, phonons are assumed to form an equilibrium bath when carrier-phonon scattering is considered. This treatment works well when the carrier system is near the equilibrium. If the carriers are far away from the equilibrium (e.g., driven by an electric field or excited by a laser beam), phonons can be driven to run away from their equilibrium states significantly by carriers when the carrier energy relaxation mainly goes through the phonon emissions and the phonon relaxation time is comparable with (or longer than) the carrier-phonon scattering time. The nonequilibrium phonons in turn are able to affect the electron dynamics, including the spin relaxation. In fact, the hot-electron transport with nonequilibrium phonons has been investigated,^{8–16} showing that the calculated electron energy loss rate and mobility fit better with experimental data than those obtained with the equilibrium phonons.^{10,13,14} These studies also indicate that it is necessary to treat phonons as nonequilibrium ones in the hot-carrier system, and the nonequilibrium phonons may affect spin relaxation via modifying the carrier heating and drifting.

The hot-electron spin relaxation/dephasing has been studied theoretically in both (001) quantum-well structures^{17–20} and bulk materials,²¹ by means of the kinetic spin Bloch equation (KSBE) approach.⁴ The spin relaxation/dephasing time is found to increase with electric field when both the temperature and electric field are low, especially in high mobility samples.^{17–21} When the electric field is high [for which the multi-subband (in confined nanostructures)¹⁸ and/or multi-valley¹⁹ effect have to be taken into account], the spin relaxation/dephasing

time decreases with electric field.^{17–19,21} In these studies the phonons are treated as equilibrium ones. This work is to investigate the influence of nonequilibrium phonons on hot-electron spin relaxation in an n -type GaAs quantum well, where the spin-orbit coupling term is the Dresselhaus type^{19,22} and the spin relaxation is limited by the D'yakonov-Perel' mechanism.⁵

The paper is organized as follows. In Sec. II we set up the model and the KSBEs with nonequilibrium phonons. In Sec. III the effect of nonequilibrium phonons on spin relaxation is investigated. Finally, we conclude in Sec. IV.

II. MODEL AND KSBES

We start our investigation from an n -type (001)|| \hat{z} GaAs quantum well with an in-plane electric field. The well width $a = 5$ nm. Only the lowest subband is relevant with the proper electron density N_e , lattice temperature T_L and electric field \mathbf{E} . Due to the electron localization in the \hat{z} -direction, the electron-phonon coupling is spatially inhomogeneous, i.e., the emission and absorption of phonons mainly occur in the well where electrons have substantial density. If the phonon relaxation is fast enough or the phonons [particularly, the acoustic (AC) phonons] can easily penetrate through the well interfaces, these phonons can be deemed as in equilibrium with the bulk modes. In our study we assume that the AC phonons keep in equilibrium and the longitudinal-optical (LO) phonons are nonequilibrium.^{9–13,15} In order to investigate the spin relaxation of electrons which are inhomogeneously coupled with the nonequilibrium LO phonons, we combine the rate equation of the LO phonons [Eq. (2)], described as “quasi-2D”,^{10,13,14} with

the electron KSBEs [Eq. (1)]:⁴

$$\frac{\partial \rho_{\mathbf{k}}}{\partial t} = \frac{\partial \rho_{\mathbf{k}}}{\partial t} \Big|_{\text{dri}} + \frac{\partial \rho_{\mathbf{k}}}{\partial t} \Big|_{\text{coh}} + \frac{\partial \rho_{\mathbf{k}}}{\partial t} \Big|_{\text{scat}}, \quad (1)$$

$$\frac{\partial n_{\mathbf{q}}}{\partial t} = \frac{\partial n_{\mathbf{q}}}{\partial t} \Big|_{\text{scat}}. \quad (2)$$

In Eq. (1), $\rho_{\mathbf{k}}$ represent the density matrices of electrons with in-plane momentum \mathbf{k} , whose diagonal terms $\rho_{\mathbf{k}\sigma\sigma} \equiv f_{\mathbf{k}\sigma}$ ($\sigma = \pm 1/2$) represent the electron distribution functions and the off-diagonal ones $\rho_{\mathbf{k}\frac{1}{2}-\frac{1}{2}} = \rho_{\mathbf{k}-\frac{1}{2}\frac{1}{2}}^*$ describe the inter-spin-band correlations for the spin coherence. $\frac{\partial \rho_{\mathbf{k}}}{\partial t} \Big|_{\text{dri}} = e\mathbf{E} \cdot \nabla_{\mathbf{k}} \rho_{\mathbf{k}}$ are the driving terms from the external electric field. $\frac{\partial \rho_{\mathbf{k}}}{\partial t} \Big|_{\text{coh}}$ are the coherent terms describing the coherent spin precessions due to the effective magnetic fields from the Dresselhaus term^{19,22} and the Hartree-Fock Coulomb interaction, as well as the optional external magnetic field in the Voigt configuration. $\frac{\partial \rho_{\mathbf{k}}}{\partial t} \Big|_{\text{scat}}$ stand for the scattering terms of electrons, including the electron-LO/AC phonon, electron-impurity and electron-electron Coulomb scatterings. $n_{\mathbf{q}}$ in Eq. (2) are the distributions of quasi-2D LO phonons with in-plane momentum \mathbf{q} . $\frac{\partial n_{\mathbf{q}}}{\partial t} \Big|_{\text{scat}}$ stand for the scattering terms of the LO phonons, including the phonon-phonon and phonon-electron scatterings. Expressions of the coherent and scattering terms of electrons are given in detail in Refs. 17 and 20, except that the electron-LO phonon scattering term should be slightly modified here as the LO phonons are described as quasi-2D (this modification makes no difference when the LO phonons are in equilibrium).^{10,13,14} The electron-LO phonon scattering term in Eq. (1) reads

$$\frac{\partial \rho_{\mathbf{k}}}{\partial t} \Big|_{\text{scat}}^{e\text{-LO}} = -\{S_{\mathbf{k}}(>, <) - S_{\mathbf{k}}(<, >) + S_{\mathbf{k}}(>, <)\}^\dagger - S_{\mathbf{k}}(<, >)\}^\dagger, \quad (3)$$

with

$$S_{\mathbf{k}}(>, <) = \frac{\pi}{A} \sum_{\mathbf{k}'} M_{\mathbf{k}-\mathbf{k}'}^2 \rho_{\mathbf{k}'}^> \rho_{\mathbf{k}}^< [n_{\mathbf{k}'-\mathbf{k}}^< \delta(\varepsilon_{\mathbf{k}} - \varepsilon_{\mathbf{k}'} + \hbar\omega_0) + n_{\mathbf{k}-\mathbf{k}'}^> \delta(\varepsilon_{\mathbf{k}} - \varepsilon_{\mathbf{k}'} - \hbar\omega_0)] \quad (4)$$

and $S_{\mathbf{k}}(<, >)$ obtained by interchanging $>$ and $<$ from $S_{\mathbf{k}}(>, <)$. The scattering term in Eq. (2) reads

$$\frac{\partial n_{\mathbf{q}}}{\partial t} \Big|_{\text{scat}} = -\frac{n_{\mathbf{q}} - n_{\mathbf{q}}^0}{\tau_{pp}} - \frac{2\pi}{A} M_{\mathbf{q}}^2 \sum_{\mathbf{k}} \delta(\varepsilon_{\mathbf{k}} - \varepsilon_{\mathbf{k}-\mathbf{q}} - \hbar\omega_0) \times [\text{Tr}(\rho_{\mathbf{k}}^> \rho_{\mathbf{k}-\mathbf{q}}^<) n_{\mathbf{q}}^< - \text{Tr}(\rho_{\mathbf{k}}^< \rho_{\mathbf{k}-\mathbf{q}}^>) n_{\mathbf{q}}^>]. \quad (5)$$

In the above equations $\rho_{\mathbf{k}}^< = \rho_{\mathbf{k}}$, $\rho_{\mathbf{k}}^> = 1 - \rho_{\mathbf{k}}$, $n_{\mathbf{q}}^< = n_{\mathbf{q}}$ and $n_{\mathbf{q}}^> = n_{\mathbf{q}} + 1$. $\varepsilon_{\mathbf{k}} = \hbar^2 \mathbf{k}^2 / 2m^*$ represents the energy of electron with momentum \mathbf{k} and effective mass $m^* = 0.067m_0$, and $\hbar\omega_0 = 35.4$ meV is the energy of the LO phonons.²³ A is the area of

the well layer. $M_{\mathbf{q}}^2 = \frac{1}{L} \sum_{q_z} g_{qq_z}^2 |I(iq_z)|^2$ is the effective electron-LO phonon scattering matrix element with $g_{qq_z}^2 = \frac{e^2 \omega_0}{2\hbar^2 \epsilon_0 (q^2 + q_z^2)} (\kappa_\infty^{-1} - \kappa_0^{-1})$.²³ L is the size of the sample along the $\hat{\mathbf{z}}$ -direction. $\kappa_0 = 12.9$ and $\kappa_\infty = 10.8$ are the relative static and high-frequency dielectric constants respectively,²³ and ϵ_0 is the vacuum dielectric constant. $|I(iq_z)|^2 = \frac{\pi^4 \sin^2 y}{y^2 (y^2 - \pi^2)^2}$ with $y = \frac{aq_z}{2}$ stands for the form factor under the infinite-depth well approximation. The first term on the right hand side of Eq. (5) represents the contribution from the phonon-phonon scattering in relaxation time approximation. $n_{\mathbf{q}}^0 = [\exp(\hbar\omega_0/k_B T_L) - 1]^{-1}$ is the number of quasi-2D LO phonons in equilibrium with the AC phonons. The population relaxation time τ_{pp} is contributed by anharmonic lattice vibrations (especially the third-order anharmonicity), which in principle depends on the phonon momentum and lattice temperature. Moreover, distinctly heated nonequilibrium LO phonons (depending on the heating and relaxation of electrons) may have different relaxation times. In spite of these intricate factors involved in the LO phonon relaxation, we assume τ_{pp} to be a constant only depending on the lattice temperature, by adopting τ_{pp} fitted by Vallée and Bogani from the time-resolved coherent anti-Stokes Raman scattering experiment.²⁴ It gives $\tau_{pp}(T_L) = \tau_{pp}^0 / \{1 + [\exp(0.2\hbar\omega_0/k_B T_L) - 1]^{-1} + [\exp(0.8\hbar\omega_0/k_B T_L) - 1]^{-1}\}$ with $\tau_{pp}^0 \equiv \tau_{pp}(0) \approx 9$ ps.²⁴ This formula in fact depicts the dominant decay route of an LO phonon near the center of the Brillouin zone into a transverse AC phonon and a different LO phonon at the L critical point of the Brillouin zone. The relaxation time approximation with a constant τ_{pp} related only to the lattice temperature has been widely utilized in the study of hot-electron transport with the presence of nonequilibrium LO phonons.¹⁰⁻¹⁴

III. RESULTS

We numerically solve the KSBEs following the scheme mainly laid out in Ref. 17, with the rate equation of the LO phonons discretized in the momentum space in a way similar to that for electrons. The impurity density is set as zero and the electric field $\mathbf{E} = -E\hat{\mathbf{x}}$ with $E \geq 0$. No magnetic field is applied except otherwise specified. The initial conditions at time $t = 0$ are chosen as the steady-state solution of Eqs. (1) and (2) in the absence of the spin-orbit coupling in the coherent term $\frac{\partial \rho_{\mathbf{k}}}{\partial t} \Big|_{\text{coh}}$.¹⁷ Numerically, they are prepared from a state at $t = -t_0$ ($t_0 > 0$) with $f_{\mathbf{k}\sigma}(-t_0) = \{\exp[(\hbar^2 \mathbf{k}^2 / 2m^* - \mu_\sigma) / k_B T_L] + 1\}^{-1}$, $\rho_{\mathbf{k}\sigma-\sigma}(-t_0) = 0$ and $n_{\mathbf{q}}(-t_0) = n_{\mathbf{q}}^0$. Here μ_σ are the electron chemical potentials determined by $\frac{1}{A} \sum_{\mathbf{k}} \text{Tr}[\rho_{\mathbf{k}}(-t_0)] = N_e$ and $\frac{1}{A} \sum_{\mathbf{k}} \text{Tr}[\rho_{\mathbf{k}}(-t_0) \sigma_z] = N_e P_0$, where $P_0 = 0.05$ is the spin polarization and $N_e = 4 \times 10^{11} \text{ cm}^{-2}$ is the electron area density. With the driving from the electric field and the scattering, the system reaches a steady

state at time $t = 0$. After time $t = 0$, the spin-orbit coupling in the coherent term is switched on and electron spins begin to relax with an initial spin polarization $P(t = 0) = P_0 = 0.05$. The spin relaxation time τ is obtained from the time evolution of spin polarization $P(t) = \frac{1}{AN_e} \sum_{\mathbf{k}} \text{Tr}[\rho_{\mathbf{k}}(t)\sigma_z]$, the electron drift velocity is the steady value of $\mathbf{v}(t) = \frac{1}{A} \sum_{\mathbf{k}} \text{Tr}[\rho_{\mathbf{k}}(t)]\hbar\mathbf{k}/m^* = v_x(t)\hat{\mathbf{x}}$ and the hot-electron temperature T_e is fitted out from the Boltzmann tail of the steady-state electron distribution.^{17,19}

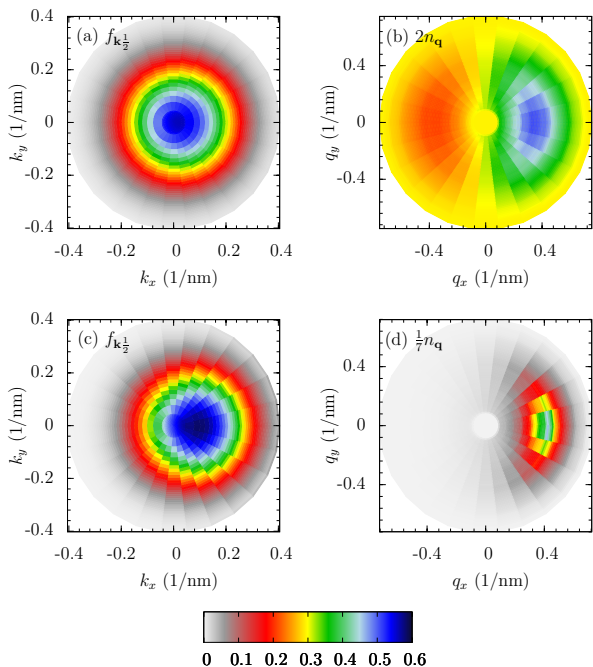


FIG. 1. (Color online) Typical steady-state distributions of nonequilibrium electrons [(a) and (c)] and LO phonons [(b) and (d)] in momentum space. (a) and (b): $T = 200$ K and $E = 0.3$ kV/cm; (c) and (d): $T = 50$ K and $E = 1$ kV/cm. Note that in (b) and (d) the LO phonon distributions $n_{\mathbf{q}}$ are rescaled by a factor 2 and $\frac{1}{7}$, respectively.

In Fig. 1 the typical steady-state distributions of the nonequilibrium electrons and LO phonons in momentum space are plotted. It is shown by Fig. 1(a) and (c) that under the electric field along the $-\hat{\mathbf{x}}$ -direction, the electrons gain a drift velocity along the $\hat{\mathbf{x}}$ -direction. Figure 1(b) and (d) show the corresponding distributions of nonequilibrium LO phonons. The LO phonons with either very large or small momenta [e.g., in the edge or center of the momentum space shown in Fig. 1(b) and (d)] are in equilibrium with the AC phonons. It is seen from the figure that the equilibrium distributions of the LO phonons are different due to the distinct lattice temperatures [200 K for Fig. 1(b) and 50 K for Fig. 1(d)]. It is interesting to see that the LO phonons with mediate momenta are driven far away from their equilibrium

states by the hot-electrons. In the case with $T_L = 200$ K and $E = 0.3$ kV/cm [Fig. 1(b)], the LO phonons with $q_x > 0$ are emitted (and form a peak in the q_x -positive momentum region) and those with $q_x < 0$ are absorbed (and form a valley in the q_x -negative momentum region). With the decrease of T_L and/or the increase of E , the valley in the q_x -negative momentum region is suppressed or even disappears, as shown in Fig. 1(d) for the case with $T_L = 50$ K and $E = 1$ kV/cm. In any case, the total phonon density increases and a net positive momentum is gained by the LO phonons.

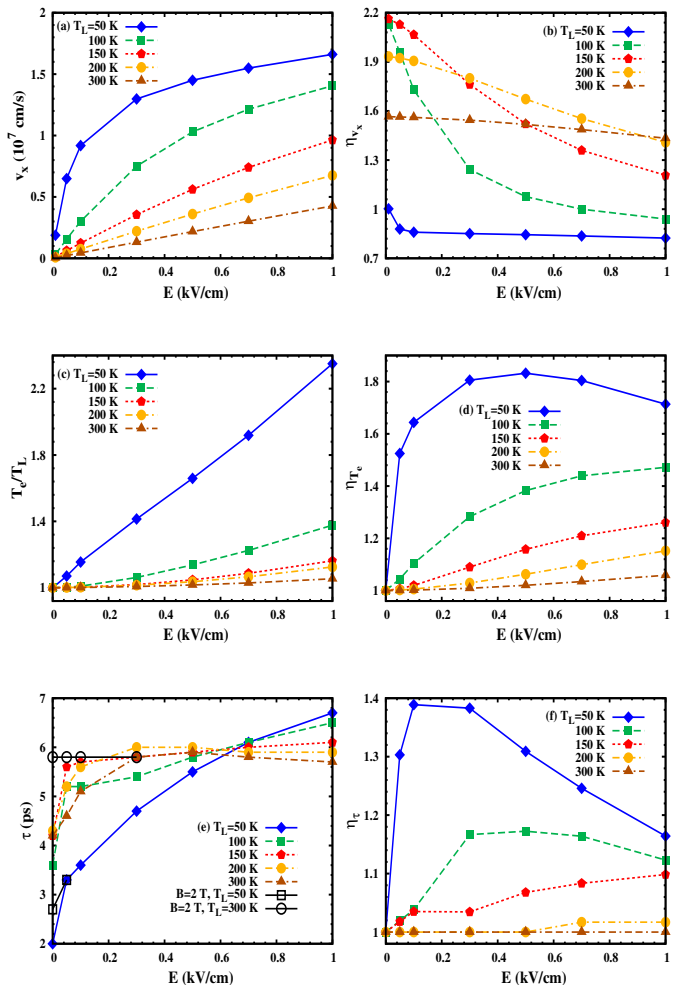


FIG. 2. (Color online) Electric field dependences of drift velocity v_x (a), hot-electron temperature T_e (c) and spin relaxation time τ (e), calculated with the equilibrium LO phonons. The ratios of the quantities v_x , T_e and τ with the nonequilibrium LO phonons to those with the equilibrium ones, η_{v_x} , η_{T_e} and η_{τ} , are shown in (b), (d) and (f), respectively. In (e), the two curves with open squares and open circles are the electric field dependences of τ with a magnetic field ($B = 2$ T) along the $-\hat{\mathbf{x}}$ -direction for $T_L = 50$ K and 300 K, respectively [at $T_L = 50$ K ($T_L = 300$ K), when $E > 0.05$ kV/cm ($E > 0.3$ kV/cm) the spin relaxation time coincides with that without magnetic field and thus not shown].

In Fig. 2(a) the electric field dependence of electron drift velocity v_x at various lattice temperatures is plotted, with the LO phonons treated as the equilibrium ones in the calculation. The ratio of v_x obtained with the nonequilibrium LO phonons to that with the equilibrium ones is shown in Fig. 2(b). From Fig. 2(b), one notices that when the nonequilibrium phonon effect is taken into account, v_x can be either increased or decreased. In fact, the influence of nonequilibrium phonons on hot-electron transport consists of two competing effects: the reabsorption of momentum from the nonequilibrium phonons tends to increase the electron mobility, while the enhanced electron heating strengthens the electron-phonon scattering (including both the electron-AC phonon and electron-LO phonon scatterings) and tends to decrease the electron mobility.^{9,11,13} Generally the former (latter) effect dominates in the regime with low (high) electric field and/or high (low) temperature,^{9,11,13} as indicated in Fig. 2(b). As mentioned previously, when the electric field is low and/or the lattice temperature is high, the valley of the LO phonon distribution in q_x -negative momentum space is pronounced, thus it substantially suppresses the back scattering of electrons in momentum space by absorbing the q_x -negative phonons and hence makes the electron distribution more forward-peaked. Finally, when the lattice temperature is high enough (e.g., $T_L = 300$ K), the effect of nonequilibrium phonons becomes weak and less sensitive to the electric field, mainly due to the shorter LO phonon relaxation time ($\tau_{pp} \approx 1.9$ ps when $T_L = 300$ K).²⁴

From Fig. 2(c), where the electric field dependence of the hot-electron temperature T_e under various lattice temperatures is shown, one indeed finds that the heating of electrons by the electric field is quite obvious when the electric field is high and the lattice temperature is low.^{17,19,21} From Fig. 2(d), where the ratio of T_e obtained with the nonequilibrium LO phonons to that with the equilibrium ones is plotted, one finds that with the nonequilibrium phonon effect considered, electrons are further heated as expected.¹¹⁻¹³ Moreover, when T_L is low, η_{T_e} shows a nonmonotonic behavior. That is caused by the decay of the heating efficiency with the increase of electric field in the presence of nonequilibrium phonons: With the increase of electric field, the number of the LO phonons increases and the rate of electron energy relaxation through the electron-LO phonon scattering increases as well. This effect is more pronounced when the lattice temperature is low, where the nonequilibrium LO phonons can be considerably accumulated with the increase of electric field, due to the long phonon relaxation time ($\tau_{pp} = 7.3$ ps when $T_L = 50$ K)²⁴ as well as the small equilibrium phonon distribution.

The electric field dependence of the spin relaxation time τ under various temperatures is plotted in Fig. 2(e). From the figure, one notices that τ generally increases with E in the regime under investigation. Two reasons lead to this phenomenon: (I) Under the electric field along the $-\hat{x}$ -direction, a net effective magnetic

field along the $-\hat{x}$ -direction is induced via the Dresselhaus spin-orbit coupling.^{17,19} With this effective magnetic field, spins begin to precess around it and thus the in-plane spin relaxation is mixed with the out-of-plane one.^{25,26} The two-dimensional electron system in (001) GaAs quantum well has an in-plane spin relaxation rate smaller than the out-of-plane one in the framework of the D'yakonov-Perel' relaxation mechanism. Thus when the electric field is applied, τ is increased due to the effective magnetic field.^{25,26} The effective magnetic field decreases with the increase of T_L , because it is proportional to v_x ^{17,19} and v_x decreases with increasing T_L [as shown in Fig. 2(a)]. Therefore the mixing of the in-plane and out-of-plane spin relaxations is obvious in the low temperature regime. In fact, when $E = 0.05$ kV/cm, the effective magnetic field is ~ 1 T when $T_L \sim 50$ -100 K and ~ 0.1 T when $T_L = 300$ K. As a result, the effective magnetic field causes an abrupt increase of τ [Ref. 25] with the increase of E from 0 to 0.05 kV/cm for the cases with $T_L \sim 50$ -100 K but a slow increase of τ with the increase of E from 0 to 0.3 kV/cm for the case with $T_L = 300$ K. (II) The heating of electrons by the electric field enhances the electron-phonon scattering and thus increases the spin relaxation time τ in the strong scattering limit.^{4,17-21} This effect, only important in the low temperature regime where the heating effect is strong [as shown in Fig. 2(c)], is responsible for the continuing increase of τ with E when $E > 0.05$ kV/cm and $T_L \sim 50$ -100 K. To make the underlying physics depicted above more pronounced, a magnetic field $B = 2$ T is applied along the $-\hat{x}$ -direction for the cases with $T_L = 50$ K and 300 K. The corresponding electric field dependences of τ are plotted as curves with open squares ($T_L = 50$ K) and open circles ($T_L = 300$ K) in Fig. 2(e). With this large external magnetic field, the in-plane and out-of-plane spin relaxations are efficiently mixed even when $E = 0$. One finds that for the case with $T_L = 300$ K, τ almost keeps unchanged with the increase of electric field, while for the case with $T_L = 50$ K τ keeps on increasing with E due to the strong heating effect. Finally, it is noted that when $T_L = 300$ K, there is a marginally decreasing tendency of τ with E when E is near 1 kV/cm. This is caused by the enhanced inhomogeneous broadening of the effective magnetic field from the Dresselhaus spin-orbit coupling due to the drifting and heating of the electric field.^{4,17-21} This effect is easier to take place when the lattice temperature is high.^{17,19}

In Fig. 2(f), the ratio of the spin relaxation time obtained with the nonequilibrium LO phonons to that with the equilibrium ones is shown. With the nonequilibrium LO phonons taken into account, τ is generally increased due to the strengthened electron-phonon scattering. Therefore the increase of τ corresponds to the increase of T_e , as shown in Fig. 2(d). However, when the lattice temperature is high enough (e.g., $T_L = 300$ K), the modification on τ induced by the nonequilibrium phonons can not be seen. Moreover, as the spin precession frequency is proportional to v_x (Refs. 17 and 19) and

v_x is affected largely by the nonequilibrium LO phonons, the spin precession frequency has a modification with the magnitude roughly proportional to the change of v_x . In Fig. 3(a) we show the typical spin precession signals with the equilibrium and nonequilibrium LO phonons, respectively. In Fig. 3(b), the typical ratio of spin precession frequency obtained with the nonequilibrium LO phonons to that with the equilibrium ones is plotted in the region of the electric field where v_x is large enough that spin precession signal with clear periods can be distinguished.

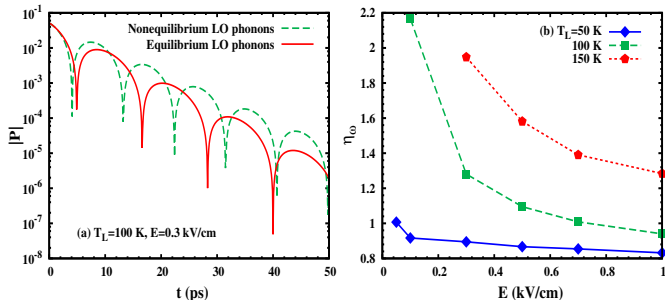


FIG. 3. (Color online) (a) Typical spin precession signals calculated with the equilibrium and nonequilibrium LO phonons. Note that the absolute value of spin polarization $|P|$ is in the logscale. $T_L = 100$ K and $E = 0.3$ kV/cm. (b) The ratio of spin precession frequency obtained with the nonequilibrium LO phonons to that with the equilibrium ones, shown at three typical temperatures in the electric field region where the spin precession signal can be clearly distinguished.

Finally, further calculations show that the effect of nonequilibrium phonons on electron mobility, electron heating and electron spin relaxation decays with the decrease of electron density and the increase of impurity density. This can be easily understood as the LO phonons are driven to the nonequilibrium states by electrons and the increase of the electron-impurity scattering suppresses the effect caused by the electron-LO phonon scattering.

IV. COUCLUSION

In this work, we have studied the effect of nonequilibrium LO phonons on hot-electron spin relaxation in n -type (001) GaAs quantum wells. Under an in-plane electric field, the LO phonons can be driven away from their equilibrium states by electrons and then in turn affect the electron transport, electron heating as well as electron spin relaxation.

In the presence of the nonequilibrium LO phonons, the electron drift velocity under electric field can be either increased (at low electric field and/or high lattice temperature) or decreased (at high electric field and/or low lattice temperature). This phenomenon is caused by the two competing effects: the momentum reabsorption from phonons and the strengthened electron-phonon scattering.^{9,11,13} The former tends to increase the electron mobility whereas the latter tends to suppress it. The nonequilibrium LO phonons also impede the energy relaxation of electrons and thus the electrons are further heated, especially when the lattice temperature is low. The nonequilibrium LO phonons effectively affect the hot-electron spin relaxation through the strengthening of the electron-phonon scattering, which tends to increase the spin relaxation time. This effect also dominates in the low temperature regime. Moreover, as the spin precession frequency under the electric field is proportional to the electron drift velocity, it can be either increased or decreased when the nonequilibrium LO phonons are taken into account. Finally, it should be noticed that the effect of nonequilibrium phonons is more pronounced in systems with high electron density and low impurity density.

ACKNOWLEDGMENTS

This work was supported by the Natural Science Foundation of China under Grant No. 10725417, the National Basic Research Program of China under Grant No. 2006CB922005 and the Knowledge Innovation Project of Chinese Academy of Sciences.

* Author to whom correspondence should be addressed; mwwu@ustc.edu.cn.

¹ D. D. Awschalom, D. Loss, and N. Samarth, *Semiconductor Spintronics and Quantum Computation* (Springer, Berlin, 2002).

² I. Žutić, J. Fabian, and S. D. Sarma, *Rev. Mod. Phys.* **76**, 323 (2004); J. Fabian, A. Matos-Abiague, C. Ertler, P. Stano, and I. Žutić, *Acta Phys. Slovaca* **57**, 565 (2007); and references therein.

³ M. I. D'yakonov, *Spin Physics in Semiconductors* (Springer, Berlin, 2008).

⁴ M. W. Wu, J. H. Jiang, and M. Q. Weng, arXiv:1001.0606; and references therein.

⁵ M. I. D'yakonov and V. I. Perel', *Zh. Éksp. Teor. Fiz.* **60**, 1954 (1971) [*Sov. Phys. JETP* **33**, 1053 (1971)].

⁶ G. L. Bir, A. G. Aronov, and G. E. Pikus, *Zh. Éksp. Teor. Fiz.* **69**, 1382 (1975) [*Sov. Phys. JETP* **42**, 705 (1976)].

⁷ R. J. Elliott, *Phys. Rev.* **96**, 266 (1954).

⁸ M. W. Wu, N. J. M. Horing, and H. L. Cui, *Phys. Rev. B* **54**, 5438 (1996).

⁹ R. Mickevičius, V. Mitin, G. Paulavičius, V. Kochelap, M. A. Stroschio, and G. J. Lafrate, *J. Appl. Phys.* **80**, 5145 (1996).

¹⁰ X. L. Lei and N. J. M. Horing, *Phys. Rev. B* **35**, 6281 (1987).

¹¹ J. C. Vaissiere, J. P. Nougier, L. Varani, P. Houlet, L.

- Hlou, L. Reggiani, and P. Kocevar, Phys. Rev. B **53**, 9886 (1996).
- ¹² J. C. Vaissiere, J. P. Nougier, M. Fadel, L. Hlou, and P. Kocevar, Phys. Rev. B **46**, 13082 (1992).
- ¹³ W. Cai, M. C. Marchetti, and M. Lax, Phys. Rev. B **37**, 2636 (1988).
- ¹⁴ W. Cai, M. C. Marchetti, and M. Lax, Phys. Rev. B **34**, 8573 (1986).
- ¹⁵ G. Paulavičius, V. V. Mitin, and N. A. Bannov, J. Appl. Phys. **82**, 5580 (1997).
- ¹⁶ M. Ramonas, A. Matulionis, and L. F. Eastman, Semicond. Sci. Technol. **22**, 875 (2007).
- ¹⁷ M. Q. Weng, M. W. Wu, and L. Jiang, Phys. Rev. B **69**, 245320 (2004).
- ¹⁸ M. Q. Weng and M. W. Wu, Phys. Rev. B **70**, 195318 (2004).
- ¹⁹ P. Zhang and M. W. Wu, Phys. Rev. B **77**, 235323 (2008).
- ²⁰ J. Zhou, J. L. Cheng, and M. W. Wu, Phys. Rev. B **75**, 045305 (2007).
- ²¹ J. H. Jiang and M. W. Wu, Phys. Rev. B **79**, 125206 (2009).
- ²² G. Dresselhaus, Phys. Rev. **100**, 580 (1955).
- ²³ X. L. Lei, D. Y. Xing, M. Liu, C. S. Ting, and J. L. Birman, Phys. Rev. B **36**, 9134 (1987).
- ²⁴ F. Vallée and F. Bogani, Phys. Rev. B **43**, 12049 (1991).
- ²⁵ J. H. Jiang, Y. Zhou, T. Korn, C. Schüller, and M. W. Wu, Phys. Rev. B **79**, 155201 (2009).
- ²⁶ S. Döhrmann, D. Hägele, J. Rudolph, M. Bichler, D. Schuh, and M. Oestreich, Phys. Rev. Lett. **93**, 147405 (2004).